International Journal of Thermophysics, Vol. 25, No. 6, November 2004 (© 2004)

Thermal Behavior of a Stagnant Gas Confined in a Horizontal Microchannel as Described by the Dual-Phase-Lag Heat Conduction Model

M. A. Al-Nimr[1,2] and A. F. Khadrawi[3]

Received March 3, 2004

The transient thermal behavior of a stagnant gas confined in a horizontal microchannel is investigated analytically under the effect of the dual-phase-lag heat conduction model. The microchannel is formed from two infinite horizontal parallel plates where the upper plate is heated isothermally and the lower one is kept adiabatic. The model that combines both the continuum approach and the possibility of slip at the boundary is adopted in this study. The effects of the Knudsen number Kn, the thermal relaxation time τ_q, and the thermal retardation time τ_T on the microchannel thermal behavior are investigated using three heat conduction models. It is found that the deviations between the predictions of the parabolic and the hyperbolic models are insignificant. On the other hand, the deviations between the parabolic and dual-phase-lag models are significant under the same operating conditions.

KEY WORDS: dual-phase-lag heat conduction model; horizontal microchannel; macroscopic heat conduction models; stagnant gas; thermal behavior.

1. INTRODUCTION

Recently, a growing interest in microchannel fluid mechanics and heat transfer has emerged because of possible cooling applications in space systems, manufacturing and material processing operations, and in high-power-density chips in supercomputers and other electronics. As this area continues to grow, it becomes increasingly important to understand the

[1]Mechanical Engineering Department, Jordan University of Science and Technology, P. O. Box 3030, Irbid 22110, Jordan.
[2]To whom correspondence should be addressed. E-mail: malnimr@just.edu.jo
[3]Mechanical Engineering Department, Al-Balqa' Applied University, Al-Salt, Jordan,

0195-928X/04/1100-1953/0

mechanisms and fundamental differences involved with fluid mechanics and heat transfer mechanisms.

It has been reported that phenomena in microgeometry may differ from those in macroscopic counterparts. Several factors that are dominant in the microscale have been identified through a number of experimental, analytical, and numerical works. Among them are the noncontinuum effect and the compressibility effect; various surface effects have been under vigorous investigation. In microgeometries the flow is described as granular for liquids and rarefied for gases, and the walls "move" [1]. The approximations for continuum flow analysis fail for microscale flows as the characteristic length of the flow gradients (L) approaches the average distance traveled by molecules between collisions (mean free path, λ). The ratio of these quantities is known as the Knudsen number ($Kn = \lambda/L$) and is used to indicate the degree of flow rarefaction or scale of the flow problem. Rarefaction or microscale effects are ignored by the Navier–Stokes equations, and these equations are therefore strictly accurate only at a vanishingly small $Kn (Kn < 0.001)$. The appropriate flow and heat transfer models depend on the range of the Knudsen number, and a classification of the different gas flow regimes is as follows: $Kn < 0.001$ for continuum flow, $0.001 < Kn < 0.1$ for slip flow, $0.1 < Kn < 10$ for transition flow, and $10 < Kn$ for free molecular flow [2].

In the slip flow regime, the continuum flow model is still valid for calculations of the flow properties away from solid boundaries. However, the boundary conditions have to be modified to account for the incomplete interaction between the gas molecules and the solid boundaries. The important features of gas flow in microducts are mainly due to rarefaction and compressibility effects. Two more effects due to acceleration and a non-parabolic velocity profile were found to be of second order compared to the effect of compressibility [3]. The rarefaction effect can be studied by solving the momentum and energy equations with slip velocity and temperature jump boundary conditions.

In spite of the large amount of published research so far in the microfluidics literature (for more details, the reader may refer to the following review papers [4, 5]), many parts of the physical laws governing the fluid flow and heat transfer in microgeometries remain unknown. Recently, discrepancies between microchannel flow behavior and macroscale Stokes flow theory have been summarized in a review [6]. It is widely accepted that the deviations observed in gas flows can be attributed to slip at the wall [7], and several researchers have reported results for gas flows [8–12].

In parallel to the breakdown of the continuum flow approach and the no-slip boundary condition from hydrodynamics and a thermal point of view, the classical diffusion energy equation, based on Fourier's law,

does not apply well in microdevices. The thermal behavior of microchannels has been extensively investigated by many researchers using different models, designs, and geometrical and operating parameters. Most of these studies are based on the parabolic (diffusion) heat conduction model. The parabolic heat conduction model is able to describe the thermal behavior of these microchannels in many practical applications. However, there are numerous cases in which the utilization of the hyperbolic or the dual-phase-lag heat conduction models becomes essential [13]. Examples of these cases are very fast transient heat conduction processes, heat conduction at cryogenic temperatures, high heating rate processes, and situations involving high temperature gradients similar to heat flow found in microsystems. In these applications, lagging is expected to occur between the heat flux and the temperature gradient across the fluid domain. Cattaneo [14] and Vernotte [15] suggested independently a modified heat flux model in the form,

$$\vec{q}(t+\bar{\tau}_q, \vec{r}) = -k\vec{\nabla}T(t, \vec{r}) \tag{1}$$

where $\vec{q}$ is the heat flux vector, k is the thermal conductivity, and $\bar{\tau}_q$ is the phase-lag in the heat flux vector. The constitutive law of Eq. (1) assumes that the heat flux vector (the effect) and the temperature gradient (the cause) across a material volume occur at different instants of time, and the time delay between the heat flux and the temperature gradient is the relaxation time $\bar{\tau}_q$. To remove the preceding assumption made in the thermal wave model, as proposed in Eq. (1), the dual-phase-lag model is proposed [16–18]. The dual-phase-lag model allows either the temperature gradient (cause) to precede the heat flux vector (effect) or the heat flux vector (cause) to precede the temperature gradient (effect) in the transient process. Mathematically, this can be represented by [19–21]

$$\vec{q}(t+\bar{\tau}_q, \vec{r}) = -k\vec{\nabla}T(t+\bar{\tau}_T, \vec{r}) \tag{2}$$

where $\bar{\tau}_T$ is the phase-lag in the temperature gradient vector and $\bar{\tau}_q$ is the phase-lag in the heat flux vector. For the case of $\bar{\tau}_T > \bar{\tau}_q$, the temperature gradient established across a material volume is a result of the heat flow, implying that the heat flux vector is the cause and the temperature gradient is the effect. For $\bar{\tau}_T < \bar{\tau}_q$, on the other hand, heat flow is induced by the temperature gradient established at an earlier time, implying that the temperature gradient is the cause, while the heat flux vector is the effect. In the absence of the temperature gradient phase-lag ($\bar{\tau}_T = 0$), Eq. (2) reduces to the classical hyperbolic heat conduction equation as described by Eq. (1). Also, in the absence of the two phase-lags ($\bar{\tau}_T = \bar{\tau}_q = 0$), Eq. (2) reduces to the classical diffusion equation employing Fourier's law. Due to

this lagging response, both the hyperbolic and dual-phase-lag heat conduction models have been receiving increasing attention as compared to the classical diffusion model, which assumes an immediate response between the heat flux vector and the temperature gradient.

The objective of this study is to investigate the microchannel transient thermal behavior under the effect of the dual-phase-lag heat conduction model. The model that combines the continuum approach with slip at the boundaries is adopted in this investigation. The effects of the Knudsen number, the phase-lag in heat flux, and the phase-lag in temperature gradients on the deviations among the three-heat conduction models are investigated.

2. ANALYSIS

Referring to Fig. 1, we consider a stagnant gas confined between two infinite horizontal parallel plates. The gas has an initial temperature T_i, and suddenly the temperature of the upper plate is raised to T_w while the lower plate is kept insulated. The gas is heated from the upper direction, and as a result, heat propagates in the downward direction by a pure conduction mode since convection currents will not be generated. Using the dimensionless parameters given in the nomenclature, the governing equations of the gas thermal behavior, as described by the dual-phase-lag heat conduction model, are given as [16]

$$\frac{\partial \theta}{\partial \eta} = -\frac{\partial Q}{\partial \xi} \tag{3}$$

$$Q + \tau_q \frac{\partial Q}{\partial \eta} = -\left(\frac{\partial \theta}{\partial \xi} + \tau_T \frac{\partial^2 \theta}{\partial \eta \partial \xi} \right) \tag{4}$$

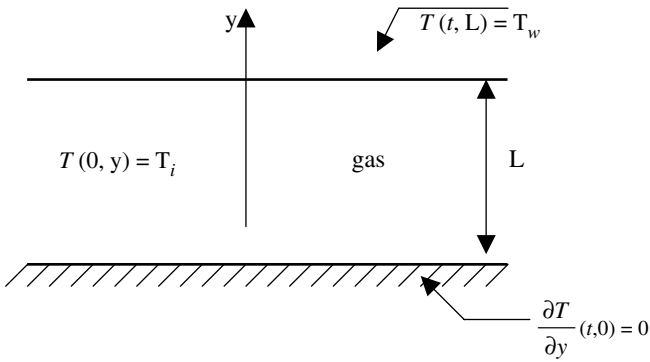

Fig. 1. Schematic diagram of the problem under consideration.

Equations (1) and (2) assume the following initial and boundary thermal conditions:

$$\theta(0,\xi) = \frac{\partial\theta}{\partial\eta}(0,\xi) = 0 \tag{5a}$$

$$\frac{\partial\theta}{\partial\xi}(\eta,0) = 0 \tag{5b}$$

$$\theta(\eta,1) - 1 = Kn\frac{\bar{\Psi}}{Pr}Q(\eta,1) \tag{5c}$$

where $\bar{\Psi} = \frac{2-\sigma_T}{\sigma_T}\left(\frac{2\gamma}{\gamma+1}\right)$ and $Kn = \frac{\lambda}{L}$ (Knudsen number)

Equation (5c) represents the temperature jump at the wall of the channel. This temperature jump is due to the lack of strong communication between the gas molecules and the wall itself. At large values of Kn, the gas mean free path length λ is relatively large, which implies that the reflected gas molecules from the wall can not gain exactly the wall energy. Also, the reflected molecules from the wall travel a long distance before collisions with other molecules so that the other molecules will not sense the exact temperature of the wall.

Equations (3)–(5) are solved using the Laplace transformation technique. Now with the notation that $L\{\theta(\tau,\xi)\} = W(S,\xi)$ and $L\{Q(\tau,\xi)\} = V(S,\xi)$, the Laplace transformation of Eqs. (3)–(5) yields

$$SW = -\frac{dV}{d\xi} \tag{6}$$

$$V + \tau_q SV = -\frac{dW}{d\xi} - \tau_T S\frac{dW}{d\xi} \tag{7}$$

Also, the Laplace transformation of the boundary conditions is given as

$$\frac{\partial W}{\partial\xi}(S,0) = 0$$

$$W(S,1) - \frac{1}{S} = Kn\frac{\bar{\Psi}}{Pr}V(S,1) \tag{8}$$

According to the boundary conditions given in Eq. (8), Eqs. (6) and (7) are solved to give

$$W = \frac{1/S}{\left[\cos h(\beta) - Kn\frac{\bar{\Psi}}{Pr}\frac{S}{\beta}\sin h(\beta)\right]}\cos h(\beta\xi) \tag{9}$$

$$V = \frac{-\sin h(\beta\xi)}{\left[\beta\cos h(\beta) - Kn\frac{\bar{\Psi}}{Pr}S\sin h(\beta)\right]} \tag{10}$$

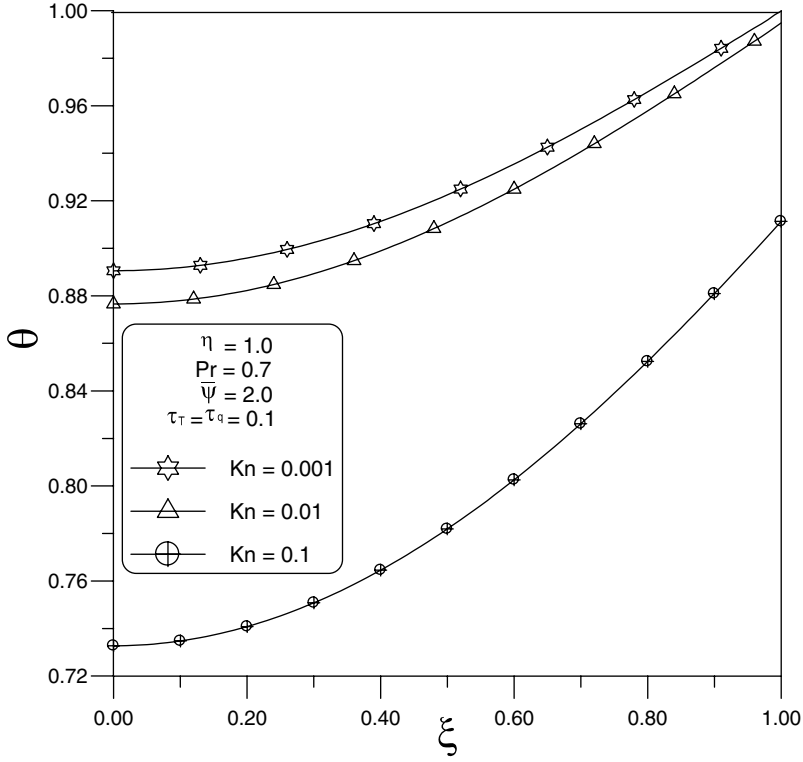

Fig. 2. Effect of the Knudsen number Kn on the dimensionless spatial temperature distribution.

where $\beta = \sqrt{\frac{S(1+\tau_q S)}{(1+\tau_T S)}}$

Equations (9) and (10) are inverted in terms of the Riemann-sum approximation [13] as

$$\theta(\eta, \xi) \cong \frac{e^{\varepsilon\eta}}{\eta}\left[\frac{1}{2}W(\varepsilon, \xi) + \mathrm{Re}\sum_{n=1}^{N} W\left(\varepsilon + \frac{in\pi}{\eta}, \xi\right)(-1)^n\right], \tag{11}$$

where Re refers to the "real part of", i is the imaginary number, and ε is the real part of the Bromwich contour that is used in inverting Laplace transforms. For faster convergence, the quantity $\varepsilon\eta = 4.7$ gives the most satisfactory results. The quantity $\varepsilon\eta = 4.7$ is found to be appropriate in our case since other tested values of $\varepsilon\eta$ seem to need longer computational time.

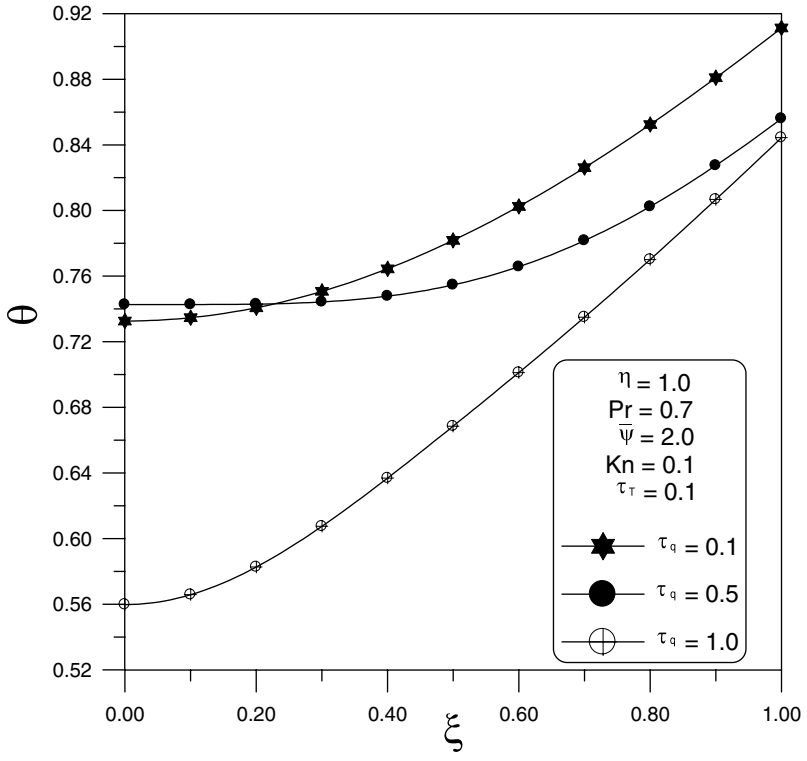

Fig. 3. Effect of the dimensionless phase-lag in the heat flux vector τ_q on the dimensionless spatial temperature distribution.

3. RESULTS AND DISCUSSION

Figure 2 shows the spatial temperature distribution at different Kn values. It is shown that as Kn increases, the temperature increases. Higher values of Kn correspond to lower values of L or higher values of the molecular mean free path λ. This implies that there are fewer molecules (high λ) in channels having a smaller width L. As a result, the heating source applied at the upper surface is able to produce higher heating effects since it has to heat a less amount of gas as Kn increases.

Figure 3 shows the effect of τ_q on the temperature spatial distribution. It is clear that this effect is more pronounced near the location of the heating source. Also, it is clear that at the same specific instant, every location attains lower temperatures as τ_q increases. As τ_q increases, the phase-lag between the heating source (the cause) and the temperature response

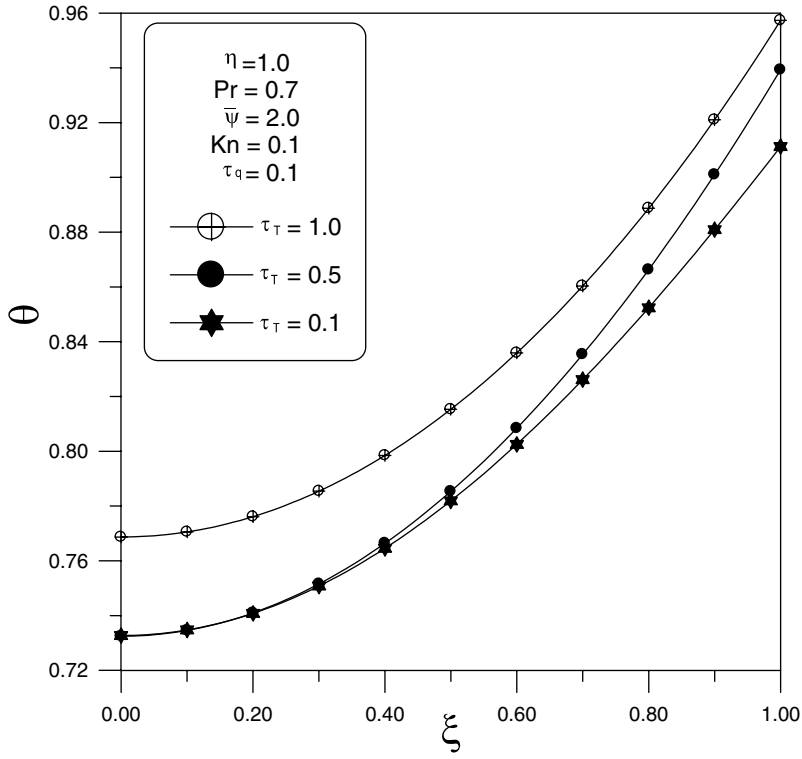

Fig. 4. Effect of the dimensionless phase-lag in the temperature gradient τ_T on the dimensionless spatial temperature distribution.

(the effect) increases. This implies that the same location attains higher temperatures as τ_q decreases.

Figure 4 shows the effect of τ_T on the spatial temperature distribution. Similar to the effect of τ_q, it is clear that the effect of τ_T is more pronounced near the location of the heating source. However, the parameter τ_T has an effect opposite to that traced for τ_q. In this case, it is clear that at the same specific instant, every location attains higher temperatures as τ_T increases. As τ_T increases, the phase-lag between the heating source (the cause) and the temperature response (the effect) decreases. This implies that the same location attains higher temperatures as τ_T increases. Figures 5 and 6 show a comparison between the parabolic heat conduction model and the hyperbolic and dual-phase-lag heat conduction models, respectively, at different Kn. It is clear from Fig. 5 that the deviations in the thermal behavior of microchannels between the parabolic

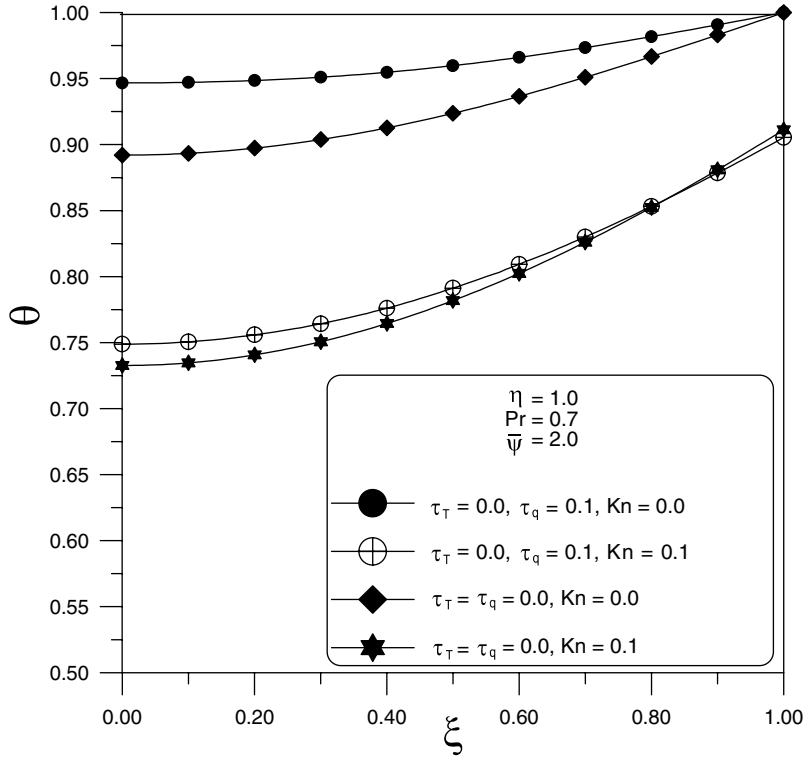

Fig. 5. Effect of the Knudsen number Kn on the dimensionless spatial temperature distribution for parabolic and hyperbolic heat conduction models.

and hyperbolic models vanish as Kn increases. This implies that both the parabolic and the hyperbolic models give the same thermal predictions in microchannels. On the other hand, the deviations between the dual-phase-lag and the parabolic models increase as Kn increases as shown in Fig. 6.

4. CONCLUSIONS

The transient thermal behavior of a stagnant gas confined in a horizontal microchannel is investigated analytically under the effect of the dual-phase-lag heat conduction model. Microchannel thermal behavior is affected by three parameters, Kn, τ_q, and τ_T. It is found that as Kn and τ_q increase, the slip in the thermal boundary condition increases. On the other hand, the parameter τ_T has an effect opposite to that traced for τ_q.

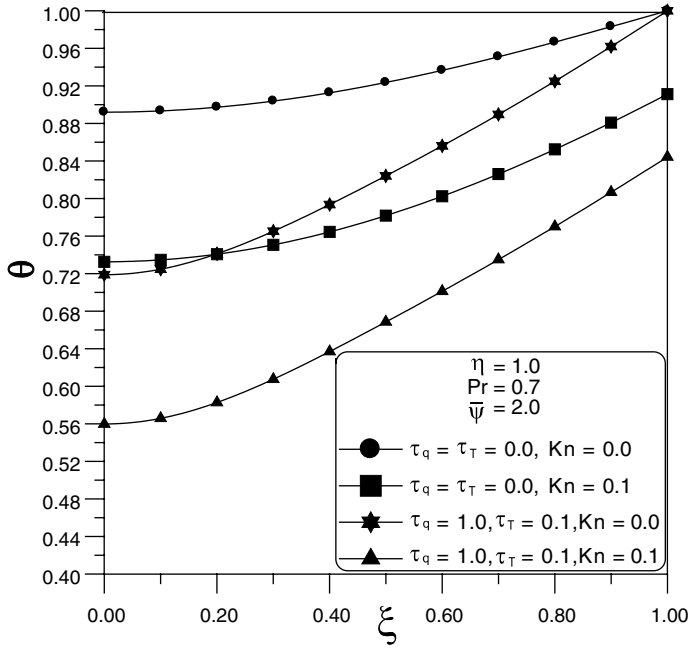

Fig. 6. Effect of the Knudsen number Kn on the dimensionless spatial temperature distribution for parabolic and dual-phase-lag heat conduction models.

NOMENCLATURE

c	specific heat, $J \cdot kg^{-1} \cdot K^{-1}$
Kn	Knudsen number, λ/L
k	thermal conductivity, $W \cdot m^{-1} \cdot K^{-1}$
L	characteristic length, m
Pr	Prandtl number, $\nu\alpha$
q	conduction heat flux, $W \cdot m^{-2}$
q_o	reference conduction heat flux, $k\Delta T/L$
Q	dimensionless conduction heat flux, q/q_o
S	Laplacian domain
t	time, s
t_o	reference time, $\Delta T \rho c L/q_o$
T	temperature, K
T_i	ambient and initial temperature, K
T_w	wall temperature, K
V	Laplace transformation of the dimensionless heat flux

W Laplace transformation of the dimensionless temperature
y transverse coordinate, m

Greek symbols

α thermal diffusivity, $m^2 \cdot s^{-1}$
ΔT dimensionless temperature difference, $T_w - T_i$
$\bar{\Psi}$ $= \frac{2-\sigma_T}{\sigma_T}\left(\frac{2\gamma}{\gamma+1}\right)$
η dimensionless time, t/t_o
γ specific heat ratio
λ mean free path, m
ν kinematic viscosity, $m^2 \cdot s^{-1}$
ρ density, $kg \cdot m^{-3}$
σ_T thermal accommodation coefficient
θ dimensionless temperature, $(T - T_i)/(T_w - T_i)$
$\bar{\tau}_T$ phase-lag in temperature gradient, s
$\bar{\tau}_q$ phase-lag in heat flux vector, s
τ_T dimensionless phase-lag in temperature gradient, $\bar{\tau}_T \alpha / L^2$
τ_q dimensionless phase-lag in heat flux vector, $\bar{\tau}_q \alpha / L^2$
ξ dimensionless transverse coordinate, y/L

Subscript

i ambient
w wall

REFERENCES

1. G. Karniadakis and A. Beskok, *Micro-flows Fundamentals and Simulation* (Springer-Verlag, New York, 2002).
2. Y. Zohar, *Heat Convection in Micro Ducts* (Kluwer, Boston, Massachusetts, 2003).
3. Y. Zohar, W. Lee, S. Lee, L. Jiang, and P. Tong, *J. Fluid Mech*. **472**:125 (2002).
4. G. P. Duncan and G. P. Peterson, *Appl. Mech. Rev*. **47**:397 (1994).
5. N. T. Obot, *Microscale Thermophy*. Eng. **6**:155 (2002).
6. C. Ho and Y. Tai, Annu. Rev. Fluid Mech. **30**:579 (1998).
7. J. C. Shih, C. Ho, J. Liu, and Y. Tai, *Microelectromech. Syst. (MEMS)* **59**:197 (1996).
8. P. Wu and W. A. Little, *Cryogenics* **23:**273 (1983).
9. S. B. Choi, R. F. Barron, and O. R. Warrington, *Micromech. Sensors, Actuators, Syst*. **32**:123 (1991).
10. J. C. Harley, Y. Huang, H. Bau, and J. N. Zemel, *J. Fluid Mech*. **284**:257 (1995).
11. S. F. Choquette, M. Faghri, E. J. Kenyon, and B. Sunden, *Proc. Nat. Heat Transfer Conf*. **5**:25 (1996).
12. Z. Y. Guo and X. B. Wu, *Int. J. Heat Transfer* **40**:3251 (1997).

13. D. Y. Tzou, *Macro to Microscale Heat Transfer, The Lagging Behavior* (Taylor and Francis, 1997), pp. 1–64.
14. C. Cattaneo, C. R. *Acad. Sci.* **247**:431 (1958).
15. P. Vernotte, C. R. *Acad. Sci*. **252**:2190 (1961).
16. D. Y. Tzou, *ASME J. Heat Transfer* **117**:8 (1995).
17. D. Y. Tzou, *Int. J. Heat Mass Transfer* **38**:3231 (1995).
18. D. Y. Tzou, *AIAA J. Thermophys. Heat Transfer* **9**:686 (1995).
19. M. A. Al-Nimr and M. Naji, *Int. J. Thermophysics* **21**:281 (2000).
20. M. A. Al-Nimr and M. Naji, *Microscale Thermophys. Eng.* **4**:231 (2000).
21. M. A. Al-Nimr, M. Naji, and V. Arpaci, *ASME J. Heat Transfer* **122**:217 (2000).